九州大学学術情報リポジトリ
Kyushu University Institutional Repository

Nanofluid-Cooled Microchannel Heat Sink with Carbon Nanotube

Hielfarith Suffri Shamsuddin
School of Mechanical Engineering, Faculty of Engineering, Universiti Teknologi Malaysia

Lee Wei Tong
School of Mechanical Engineering, Faculty of Engineering, Universiti Teknologi Malaysia

Normah Mohd-Ghazali
School of Mechanical Engineering, Faculty of Engineering, Universiti Teknologi Malaysia

Patrice Estellé
Univ Rennes

他

https://doi.org/10.5109/4372274

出版情報：Evergreen. 8 (1), pp.170-176, 2021-03. Transdisciplinary Research and Education Center for Green Technologies, Kyushu University
バージョン：
権利関係：

KYUSHU UNIVERSITY

Nanofluid-Cooled Microchannel Heat Sink with Carbon Nanotube

Hielfarith Suffri Shamsuddin[1], Lee Wei Tong[2], Normah Mohd-Ghazali[3,*], Patrice Estellé[4], Thierry Maré[5], and Maziah Mohamad[6]

[1,2,3,6]School of Mechanical Engineering, Faculty of Engineering
Universiti Teknologi Malaysia, 81310 Skudai, Johor, Malaysia
[4,5]Univ Rennes, LGCGM, 35000 Rennes, France.

*Author to whom correspondence should be addressed:
E-mail: normah@mail.fkm.utm.my

(Received November 27, 2020; Revised February 19, 2021; accepted March 23, 2021).

Abstract: Concerns over the exponential increase in the heat produced per unit area in electronic chips have driven advanced research into the nanofluid capability as a coolant. Generally reported for its improved thermal conductivity in particular at higher concentrations, different types of surfactant normally added used to stabilize the nanofluid have reported different thermal resistance to heat flow. This paper reports an analysis of the thermal performance of a nanofuid-cooled microchannel heat sink (MCHS) with 0.1% volume fraction of CNT nanofluid utilizing two different surfactants; Lignin (N2) and sodium polycarboxylate (N3) as stabilizers. Multi-objective particle swarm optimization (MOPSO) algorithm was utilized to simultaneously minimize the thermal resistance and pumping power by optimizing the design parameters; the wall width and channel aspect ratios. Optimization outcomes showed that the thermal resistance of CNT nanofluids is lower than water by 1% at 20°C. Nanofluid with N3 has a significantly higher pressure drop than water, up to 47%. CNT nanofluid with N3 performed poorly due to the high viscosity which consequently results both in higher thermal resistance and pressure drop. Since a surfactant alters the properties of nanofluid, it could improve or deteriorate the performance of a MCHS overall and must not be taken lightly as a MCHS is expected to operate for a long time.

Keywords: microchannel heat sink; nanofluid; lignin; carbon nanotubes; sodium polycarboxylate

1. Introduction

Heat sink is an effective heat removal system used to remove unwanted heat from a generating source such as electronic chips from computers. The first micro-sized physical cooling system of a heat sink was proposed by Tuckerman and Pease in 1981[1)]. They promoted water as a coolant flowing in laminar flow in a silicon microchannel heat sink (MCHS) to eliminate high heat loads. The coolant of a MCHS since its emergence, have moved to air, oil, ethane and more, depending on its application. In the current century, the size of the modern technology electronic chips has become smaller while the power density has exponentially increased as the industry moved to miniaturization and digitalization. The design of a good thermal management system to carry heat away from the electronic chips becomes a major concern in this electronic industry. To some extend for extreme heat load, the flow condition in a MCHS may evolve from a single phase into two-phase where both liquid and gas are present in the system with the highest thermal performance driven by maximizing convection and minimizing entropy generation[2)].

Water as liquid coolant would not be adequate to perform effective cooling of the MCHS for future practices. To further improve the thermal performance, nanofluid is promoted to increase the rate of heat transfer. Nanofluid is generally comprised of a base fluid such as water, ethylene glycol, or oil, and nanoparticles typically made of oxides, metals, nitrides, carbides, or carbon materials such as carbon nanotubes (CNT). In 2007, the first ever nanofluid-cooled rectangular MCHS with CNT was proposed by Tsai and Chein[3)]. CNT is considered as a new material during these few decades not only in a MCHS but also as lubricants[4,5)] with its current production technology being explored such as flame synthesis[6)], two-step cascade process[7)] and laminar hydrogen/air flames streaming[8)]. Tsai and Chein[3)] demonstrated that the coolant CNT-water with 2% and 4 % volume fraction of nanotube provided a better heat transfer than pure water

which is 0.0657 K/W and 0.086 K/W respectively. Adham et al[9] reported that nanofluid achieved a lower thermal resistance compared to pure water. These nanoparticles increase the thermal conductivity of a working fluid, thus enhancing its thermal performance.

Halelfadl et al.[10] used the thermal resistance model and concluded that CNT nanofluid with surfactant sodium dodecyl benzoic sulfate (SDBS) reduced the thermal resistance and improved significantly the thermal performance of a MCHS at high temperature[10]. The optimized thermal resistance for their CNT nanofluid tested performed better than water at high temperature by enhancing the cooling performance. However, the nanofluid is generally unstable and the presence of a surfactant is necessary to prevent agglomeration of the nanoparticles[11,12]. Ruliandini[13] reported that agglomeration occurs due to the Van der Waals forces and instability in the nanofluid will not produce the desired improved heat transfer performance[13]. Surfactants are an important ingredient to stabilize a nanofluid and their effect have often been neglected during investigations of the enhancement outcomes of a nanofluid[14]. Thus, any study involving a particular nanofluid should explicitly state the type of surfactant used. In the current study, the performance of similar CNT used to produce nanofluids with two types surfactants, Lignin (N2) and Sodium Polycarboxylate (N3)[15] were investigated with a MCHS design of Tuckerman and Pease[1].

It has been generally agreed that the reduction in the thermal resistance will result in an increase in the pressure drop and vice versa. In order to achieve a high performance thermally and hydrodynamically, both performance parameters must be as low as possible. The importance of decreasing the pressure drop is crucial as it reduces the energy consumption of the system via pumping power which contributes to energy demand reduction. New technology must always be accompanied with considerations towards energy savings in order to move to the digitalization era and a sustainable society[16]. Therefore, optimization, the process of identifying the best solution from among several possible solutions, is required especially when conflicting objectives are involved[17,18]; social[19], economic[20,21,22], physical[23], and technological[24,25] constraints.

In this study, outcomes of the simultaneous minimization of the thermal resistance and pressure drop of a rectangular MCHS using aqueous carbon nanotubes based nanofluid, with N2 and N3 surfactants, are reported. Though there are many optimization methods available for designs to achieve multiple objectives for heat exchangers[18], there are two optimization tools which have been found to be relevant for a MCHS:

a) Multi-Objective Genetic Algorithm (MOGA)[9]
b) Multi-Objective Particle Swarm Optimization (MOPSO)[15]

MOGA has been widely used in a MCHS optimization compared to MOPSO. However, it has been clearly shown that with the same parameters, Mohd-Ghazali et al.[15] have attained better optimization results with MOPSO. They also found that the optimum volume fraction for nanofluid CNT is only 0.1%, any higher will result in an overwhelming increase in the pressure drop. Thus, in this study MOPSO is used in optimizing the parameters of a MCHS with the studied nanofluids. The bulk properties are shown in Table 1. It is observed in the Table that main difference between both nanofluids come from viscosity values. Such a difference is attributed to the dispersion state of CNT that is linked to the type of surfactant.

Table 1: Bulk properties at 20°C of 0.1%vf CNT nanofluids with different surfactants[15]

	Lignin (N2)	Sodium Polycarboxylate (N3)
Thermal conductivity, k_f (W/m.K)	0.62392	0.62392
Density, ρ (kg/m^3)	1001.29	1001.29
Heat Capacity C_p (J/kg.K)	4175.021	4175.021
Dynamic viscosity, μ_f (Ns/m^2)	0.00107259	0.00138372

2. Methodology

2.1 Mathematical Model

Fig. 1 shows a schematic of a MCHS with rectangular microchannels identical with that experimented by Tuckerman and Pease[1]. For this modelling, a uniform heat flux boundary condition is assumed to be at the lowest point of the MCHS where the microchip highest surface will be in contact. Coolant is pumped through the microchannels via a micropump and a cover plate covers the top of the MCHS with the system assumed to be adiabatic. The thermal performance of a MCHS is represented by its thermal resistance. The material used for the heat sink is silicon.

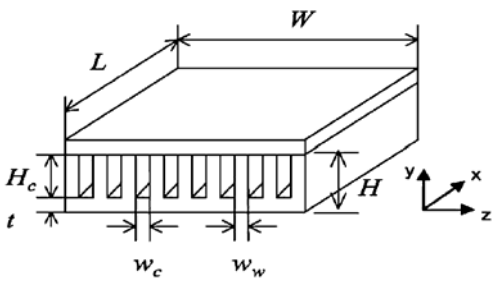

Fig. 1: Schematic structure of rectangular cross section MCHS[9]

The design parameters are the width of the MCHS, *W*, height of the MCHS, *H*, length of the MCHS, *L*, thickness

of the substrate, t, channel height, H_c, channel width, w_c, and wall width, w_w. To determine the thermal performance of a nanofluid-cooled MCHS, the model system is evaluated and optimized using the total thermal resistance equation of Adham et al.[9]. The thermal resistance model shown in Eq. 1 is able to assess the thermal performance of the heat sink system. Since the device utilized the design of a microchannel, the flow of coolant and its capability as a heat transporter, the total thermal resistance of all heat transfer categories must be evaluated:

$$R_{total} = R_{conductive} + R_{convective} + R_{capacitive} \quad (1)$$

The three conductive, convective, and capacitance resistances were evaluated to determine the thermal performance of the MCHS. Heat flux from the heat source flows through the substrate whose resistance is calculated with Eq. 2 through conductive resistance to the microchannel. Once the heat reaches the microchannel, it is then transferred to the coolant either from the substrate highest point or through the wall between the microchannel which in Eq. 3 is assumed as fin here[10]. Eq. 4 is the heat being removed following the capability of the coolant to store heat which is measured with the capacitive thermal resistance. All three types of heat transfer thermal resistance are defined as:

$$R_{conductive} = \frac{t}{k_{hs}} \quad (2)$$

$$R_{convective} = \frac{1}{h_{av}} \frac{1+\beta}{1+2\alpha n} \quad (3)$$

$$R_{capacitive} = \frac{L}{C_{pnf}\mu_{nf}} \frac{2}{\mathrm{Re}} \frac{1+\beta}{1+\alpha} \quad (4)$$

The resistances are then combined as the total thermal resistance as in Eq. 1.

The hydrodynamic performance is represented by the pressure drop, Δp, of the microchannel as well as the pumping power, P_p:

$$\Delta p = \Delta p_1 + (\Delta p_2)(\Delta p_3) \quad (5)$$

$$\Delta p_1 = f \frac{(1+\alpha)L}{2H_c} \rho_f \frac{V^2}{2} \quad (6)$$

$$\Delta p_2 = (\Delta p_{2a} + \Delta p_{2b}) \quad (7)$$

$$\Delta p_{2a} = 1.79 - 2.23\left(\frac{1}{1+\beta}\right) \quad (8)$$

$$\Delta p_{2b} = 0.53\left(\frac{1}{1+\beta}\right)^2 \quad (9)$$

$$\Delta p_3 = \rho_f \frac{V^2}{2} \quad (10)$$

$$P_p = \Delta p \times G \quad (11)$$

In the optimization process, the channel aspect ratio, α, and wall width ratio, β, are the keys to manage the design variables for a maximum optimized thermal performance of a MCHS and described as:

$$\alpha = \frac{H_c}{w_c} \quad (12)$$

$$\beta = \frac{w_w}{w_c} \quad (13)$$

2.2 Mathematical Model Validation

According to Table 2 which is the validation of the model used with the experimental results of Tuckerman and Pease[1], the relative difference of the thermal resistance and pressure drop is 5.8% and 3.5% respectively, showing that the model has a good accuracy with the experimental results. The deviation could be caused by the different properties of the coolant as Tuckerman and Pease[1] used deionized water at 23°C, while here 20°C was presently considered. The slight difference in the properties could have caused the deviations.

Table 2: Mathematical model validation

Parameters	**Tuckerman and Pease[1]**	**Current Model**
W (m)	0.01	0.01
L (m)	0.01	0.01
H_c (m)	0.00032	0.00032
α	5.7143	5.7143
β	0.7857	0.7857
R_{th} (K/W)	0.110	0.104
ΔP (kPa)	103.4	107.01
P_p (W)	0.49	0.50
Relative uncertainty		
R_{th} (%)	-	5.8
ΔP (%)	-	3.5

2.3 Optimization

The optimization method of Multi-Objective Particle Swarm optimization (MOPSO) is referenced from Mohammad[26]. The manipulated variables are α and β with its boundary set by 3.2 to 32 and 1 to 10 respectively to limit w_c and w_w.

Utilizing the same design parameters of Tuckerman and Pease[1], the optimization was carried out and the outcomes shown in Table 3.

Table 3: Optimization with water and compared to non-optimized water

	Non-optimized	Optimized
α	5.71	6.32
β	0.79	0.23
w_c (μm)	56	50.6
w_w (μm)	44	13.6
R_{th} (K/W)	0.104	0.100
ΔP (kPa)	107	90.5
P_p (W)	0.50	0.43
$\Delta R_{th}/R_{th}$	-	3.8%
$\Delta P_p/P_p$	-	15.4%
Constant Variables		
H_c (μm)	320	
t (μm)	213	
G (cm^3/s)	4.7	

The channel height, substrate thickness and the flow rate were kept constant according to the experimental values. Simultaneous optimization has been done for the minimization of the thermal resistance and pressure drop. The possible solutions were able to lower both the thermal resistance and pressure drop of water by 3.8% and 15.4%, respectively. MOPSO method is capable to find the optimum design parameters to improve the MCHS according to the coolant's properties.

3. Results and Discussion

With the same design parameters of that Tuckerman and Pease[1], the thermophysical properties in Table 1 was extracted into the model to predict its performance and tabulated into Table 4.

Table 4: MCHS performance with CNT nanofluids with different surfactant, N2 and N3, at 20°C compared to water.

	Non - optimized	
	N2	N3
α	5.71	5.71
β	0.79	0.79
w_c (μm)	56	56
w_w (μm)	44	44
R_{th} (K/W)	0.1025	0.1025
ΔP (kPa)	122	157
P_p (W)	0.58	0.74
$\Delta R_{th}/R_{th}$	-1%	-1%
$\Delta P_p/P_p$	14%	47%
Constant Variables		
H_c (μm)	320	
t (μm)	213	
G (cm^3/s)	4.7	

N3, with sodium polycarboxylate surfactant has a higher pumping power than N2, with lignin, which can be seen in Table 4. Since the nanofluid is mixed with a different surfactant, the viscosity has a significant difference although both CNT nanofluids, herewith referred to as N2 and N3, have the same other thermophysical properties. Due to this, N3 obtained a higher pressure drop as much as 35kPa difference compared to N2 as it is directly affected by viscosity. The viscosity affects directly with friction factor, which results in N2 having a lower pumping power than N3. Although the thermal resistance is the same, the pressure drop will definitely affect the thermal resistance in the optimization process as MOPSO considered both objectives to be attained simultaneously. Fig. 2 shows the sets solutions (pareto front) of optimization of N2 and N3.

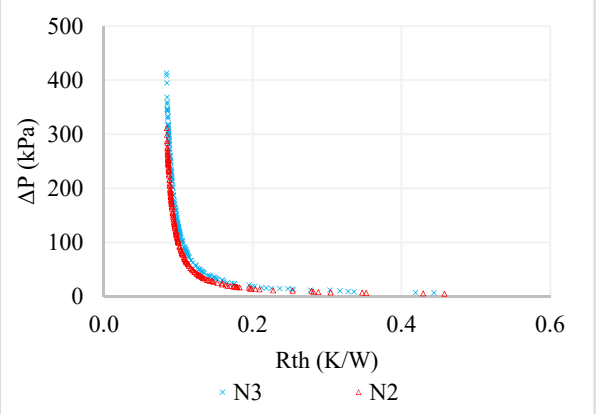

Fig. 2: Optimized pumping power against total thermal resistance for water and CNT nanofluids at 20°C

Figure 2 shows the consequence of reducing the thermal resistance as the pressure drop increases. Each point in the graph is the result of solutions for optimized thermal and hydrodynamic performance according to the limitation that has been programmed in MOPSO. N2 nanofluid performs better than N3 because the pareto front of N3 is higher compared to N2. N3 surfactant affected the viscosity causing a higher thermal resistance and pressure drop compared to N2. Therefore, only one point of possible solution with the same pressure drop was chosen for comparison in Table 5.

Table 5: Optimized CNT nanofluid N2 and N3 and comparison to non-optimized.

	Optimized	
	N2	**N3**
α	6.38	6.28
β	0.32	0.31
w_c (μm)	50.2	51.0
w_w (μm)	15.9	15.8
R_{th} (K/W)	0.098	0.099
ΔP (kPa)	110	136
P_p (W)	0.50	0.63
$\Delta R_{th}/R_{th}$	-4.3%	-3.6%
$\Delta P_p/P_p$	-10%	-13%
	Constant Variables	
H_c (μm)	320	
t (μm)	213	
G (cm^3/s)	4.7	

Simultaneous optimization has been done for both CNT nanofluids, N2 and N3. Reduction of thermal resistance and pressure drop by 4.3% and 10% could be achieved by CNT nanofluid with lignin as surfactant. With optimization, CNT nanofluid with Sodium polycarboxylate, the reduction in its pressure drop is higher, by 13%. However, to compensate for the high pressure drop due to viscosity, it is impossible to achieve thermal resistance any better than CNT nanofluid N2. Both optimized CNT nanofluids have lowered the thermal resistance and pressure drop, but since surfactant Sodium polycarboxylate has resulted in a higher viscosity in the CNT nanofluid, its pressure drop and thermal resistance was larger than N2 even after being optimized. With the results of N2, a lower viscosity in the MCHS system also enables to further reduce the system's thermal resistance.

Optimization is a desirable process to find the design variable, dimensions, to reduce both the thermal resistance and pressure drop in a MCHS. But even with the change of only viscosity due to the presence of a surfactant with no difference in thermal conductivity, it jeopardized the overall performance of the system after being optimized. A surfactant that increases the nanofluid viscosity will result in a higher thermal resistance as the geometry were adjusted according to the properties that caused the desired heat removal capability. Therefore, the effects of different types of surfactant should be taken into consideration when utilizing nanofluids for a MCHS coolant. This study shows that with the same type of nanoparticles or nanotubes in a nanofluid, different surfactants effects must be investigated as they change the properties of the nanofluid due to difference in dispersion state. Hence, it will dramatically alter the impact of using a nanofluid specifically for MCHS cooling applications.

4. Conclusion

The thermal performances of a MCHS cooled with CNT nanofluid containing different surfactants which are Lignin (N2) and Sodium polycarboxylate (N3) have been completed utilizing MOPSO. With the same volume fraction of 0.1%, nanofluid with N2 surpasses that with N3 in the hydrodynamic performance due to a lower pressure drop or pumping power necessary to achieve the same heat removal capacity. With difference in viscosity, CNT nanofluid N2 and N3 were able to further reduce the thermal resistance by 4.3% and 3.6% respectively through optimization. Thermal resistance of optimized CNT nanofluid N3 was only able to reduce by 3.6% to compensate for its lower pressure drop. It has reduced the pressure drop by 13% while CNT nanofluid N2 was only reduced by 10%. Nevertheless, both thermal resistance and pressure drop of the CNT nanofluid N2 is lower than CNT nanofluid N3. For current findings, lignin surfactant was proven to be a better stabilizer for CNT nanofluid as compared to Sodium polycarboxylate. Further studies need to be done to look over more types of surfactants for better a performance in applications involving MCHS coolants with CNT nanofluids. The effects of surfactants towards the properties of CNT nanofluid have significantly influenced the MCHS performance which therefore must be investigated thoroughly since a MCHS cooling ability is dependent on the coolant's stability over long durations of application of nanofluids.

Acknowledgements

The authors acknowledge the funding from the Research University Grant Universiti Teknologi Malaysia, GUP Vot 19H60 and the Malaysian French Embassy, to complete this research.

Nomenclature

C_p	Heat capacity (J/kg.K)
f	Friction factor
G	Volumetric flow rate (m^3/s)
h	Height (m)
h_{av}	Heat transfer coefficient ($W/m^2 \cdot K$)
k	Thermal conductivity (W/m·K)
L	Length (m)
P_p	Pumping power (W)
R	Thermal resistance (K/W)
Re	Reynolds number
t	Substrate thickness (m)
V	Velocity (m/s)
W,w	Width (m)

Greek symbols

μ	Dynamic viscosity (kg/s·m)
α	Channel aspect ratio
β	Wall width ratio
n	Fin efficiency
Δp	Pressure drop (Pa)
ρ	Density (kg/m^3)

Subscript

c	Channel
f	Fluid
hs	Heat sink
nf	Nanofluid
w	wall

References

1) D.B. Tuckerman, and R.F.W. Pease, "High-performance heat sinking for VLSI," *IEEE Electron Device Letters*, **2** *(5)* 126-129 (1981). doi: 10.1109/EDL.1981.25367.
2) A.S. Syahrul, J.T. Oh, N. Mohd-Ghazali, A. Robiah, and Y. Mohd-Yunos, "Entropy Generation Minimization of Two-Phase Flow in a Mini Channel with Genetic Algorithm," *Evergreen*, **6** *(1)* 39-43 (2019). doi:10.5109/2321004.
3) T.H. Tsai, and R. Chein, "Performance analysis of nanofluid-cooled microchannel heat sinks," *International Journal of Heat and Fluid Flow*, **28** *(5)* 1013-1026 (2007). doi:10.1016/j.ijheatfluid flow.2007.01.007.
4) H. Pourpasha, S. Zeinali Heris, O. Mahian, and S. Wongwises, "The effect of multi-wall carbon nanotubes/turbine meter oil nanofluid concentration on the thermophysical properties of lubricants," *Powder Technology,* **367** 133-142 (2020). doi:10.1016/j.powtec.2020.03.037.
5) E. Ettefaghi, H. Ahmadi, A. Rashidi, A. Nouralishahi, and S.S. Mohtasebi," Preparation and thermal properties of oil-based nanofluid from multi-walled carbon nanotubes and engine oil as nano-lubricant," *International Communications in Heat and Mass Transfer,"* **46** 142-147 (2013). doi:10.1016/j.icheatmasstransfer.2013.05.003.
6) N. Hamzah, M.F. Mohd Yasin, M.Z. M. Yusop, and M.T. Zainal, "Identification of CNT Growth Region and Optimum Time for Catalyst Oxidation: Experimental and Modelling Studies of Flame Synthesis," *Evergreen,* **6** *(1)* 85-91 (2019). doi:10.5109/2328409.
7) L. Qiang, W. Pan, H. Jian, L. Changjun, and J. Wei, "Catalytic decomposition of methane by two-step cascade catalytic process: Simultaneous production of hydrogen and carbon nanotubes," *Chemical Engineering Research and Design*, **163** 96-106 (2020). doi:10.1016/j.cherd.2020.08.029.
8) Z. Cen, T. Bo, T.C. Cheng, D. Boning, F. Luming, C. Xin, and S. Hochgreb, "Synthesis of single-walled carbon nanotubes in rich hydrogen/air flames," *Materials Chemistry and Physics*, ***254*** (2020).doi:10.1016/j.matchemphys.2020.123479.
9) A.M. Adham, N. Mohd-Ghazali, and R. Ahmad, "Optimization of Nanofluid-cooled microchannel heat sink," *Thermal Science*, **20** *(1)* 109-118 (2016). doi:10.2298/TSCI130517163A.
10) S. Halelfadl, A.M. Adham, N. Mohd-Ghazali, T. Mare, P. Estelle, and R. Ahmad, "Optimization of thermal performances and pressure drop of rectangular microchannel heat sink using aqueous carbon nanotubes based nanofluid," *Applied Thermal Engineering*, **62** *(2)* 492-499 (2014). doi:10.1016/j.applthermaleng.2013.08.005.
11) H. Garg, V.S. Negi, N. Garg, and A.K. Lall, "Numerical and experimental analysis of microchannel heat transfer for nanoliquid coolant using different shapes and geometries," *Proceedings of the Institution of Mechanical Engineers, Part C: Journal of Mechanical Engineering Science,* **229** *(11)* 2056-2065 (2014). doi:10.1177/0954406214550846.
12) R. Kamali, Y. Jalali, and A.R. Binesh, "Investigation of multiwall carbon nanotube-based nanofluid advantages in microchannel heat sinks," *Micro and Nano Letters,* **8** *(6)* 319-323 (2013). doi:10.1049/mnl.2012.0803.
13) R. Ruliandini, Nasruddin, and T. Tokumasu, "Assessing hBN Nanoparticles Stability in Trimethylolpropane Triester Based Biolubricants Using Molecular Dynamic Simulation," *Evergreen*, **7** *(2)* 234-239 (2020). doi:10.5109/4055225,
14) Y. Xuan, Q. Li, and P. Tie, "The effect of surfactants on heat transfer feature of nanofluids," *Experimental Thermal and Fluid and Fluid Science*, **46** 259-262 (2013). doi:10.1016/j.expthermflusci.2012.12.004.
15) N. Mohd-Ghazali, P. Estellé, S. Halelfadl, T. Maré, C. S. Tng, and U. Abidin, "Thermal and hydrodynamic performance of a microchannel heat sink with carbon

nanotube nanofluids," *Journal of Thermal Analysis and Calorimetry,* **138** *(2)* 937-945 (2019). doi:10.1007/s10973-019-08260-2.

16) M. Barai, and B. Saha, "Energy Security and Sustainability in Japan," *Evergreen Joint J Nov Carbon Resource Science Green Asia Strategy,* **2** *(1)* 49-56 (2015). doi:10.5109/1500427.
17) M.I. Hamid, N. Nasruddin, Budihardjo, and E. Susanto, "Refrigeration Cycle Exergy-Based Analysis of Hydrocarbon (R600a) Refrigerant for Optimization of Household Refrigerator," *Evergreen*, **6** *(1)* 71-77 (2019). doi: 10.5109/2321015.
18) Y.D. Kim, K. Thu, and C.N. Kim, "Evaluation and Parametric Optimization of the Thermal Performance and Cost Effectiveness of Active-Indirect Solar Hot Water Plants," *Evergreen,* **2** *(2)* 50-60 (2015). doi:10.5109/1544080.
19) L. Messmann, V. Zender, A. Thorenz, and A. Tuma, "How to quantify social impacts in strategic supply chain optimization: State of the art," *Journal of Cleaner Production,* **257** **(**2020). doi:10.1016/j.jclepro.2020.120459.
20) S. Yuanyuan, M. Xianqiang, L. Gengyuan, Y. Xinan, and Z. Yanwei, "Greener economic development via carbon taxation scheme optimization," *Journal of Cleaner Production*, **275** (2020). doi:10.1016/j.jclepro.2020.124100.
21) M. Momen, M. Shirinbakhsh, A. Baniassadi, and A. Behbahani-nia, "Application of Monte Carlo method in economic optimization of cogeneration systems – Case study of the CGAM system," *Applied Thermal Engineering*, **104** 34-41 (2016). doi:10.1016/j.applthermaleng.2016.04.149.
22) A.M.A. Haidar, A. Fakhar, and A. Helwig, "Sustainable energy planning for cost minimization of autonomous hybrid microgrid using combined multi-objective optimization algorithm," *Sustainable Cities and Society*, **62** (2020). doi:10.1016/j.scs.2020.102391.
23) A.B. Awan, K.V.V. Chandra Mouli, and M. Zubair, "Performance enhancement of solar tower power plant: A multi-objective optimization approach," *Energy Conversion and Management*, **225** (2020). doi:10.1016/j.enconman.2020.113378.
24) Z. Yan, J. Zhang, and J. Tang, "Path planning for autonomous underwater vehicle based on an enhanced water wave optimization algorithm," *Mathematics and Computers in Simulation,* ***181*** 192-241 (2020). doi:10.1016/j.matcom.2020.09.019.
25) G. Valencia, A. Fontalvo, and J. Duarte-Forero, "Optimization of Waste Heat Recovery in Internal Combustion Engine Using A Dual-Loop Organic Rankine Cycle: Thermo-Economic And Environmental Footprint Analysis," *Applied Thermal Engineering,* ***182*** (2020). doi:10.1016/j.applthermaleng.2020.116109.
26) M. Mohammad, "Intelligence modelling and active vibration control of flexible structures," Phd Thesis, University of Sheffield, 2011.